Plasma resonances in thin Bi films

L. M. Claessen,* A. G. M. Jansen,* and P. Wyder*
Research Institute for Materials, University of Nijmegen, Toernooiveld, NL-6525 ED Nijmegen, The Netherlands
(Received 7 June 1985; revised manuscript received 2 December 1985)

The optical absorption and transmission of thin Bi films (50—830 nm) illuminated with normally incident far-infrared radiation (25—225 cm^{-1}) have been measured at low temperatures ($T=1.5$ K). Around the theoretical screened-electron plasma frequency (160—170 cm^{-1}) a broad absorption band has been observed which disappeared for films thinner than 200 nm. This phenomenon will be visualized in terms of a virtual-mode excitation of the electron gas undergoing strong radiation damping. An electrodynamical analysis of a thin conducting film reveals that a Drude approximation for the conduction electrons is not sufficient to explain the experimental results in detail. Deviations from this model are discussed in terms of two-phonon processes and electron—ionized-impurity scattering.

I. INTRODUCTION

The plasma frequency of the conduction electrons is defined as the frequency ω for which the dielectric function $\epsilon(\omega)$ equals zero.[1] In semiconductors and semimetals, this frequency is situated below the visible frequency region owing to a very small electron density. In these materials, plasmons can therefore be investigated in a spectral region for which local relations and the Drude approximation prevail.[2,3]

In the semimetal Bi, the plasma frequency[4] is situated in the far-infrared at about 160 cm^{-1}. Since in semiconductors the optical-phonon frequencies are often in the same spectral region as the free-electron contributions, discerning between different absorption mechanisms can be difficult. In Bi, however, the optical phonons are infrared inactive[5,6] owing to the crystal symmetry, which leaves the free-electron absorption as the most important mechanism.

Using a normally incident light source as a probe for the free-electron excitations, it is in general not possible to excite plasmons (i.e., longitudinal excitations) in the electron gas in a direct way. Only by intervention of a rough surface[7,8] or of ionized impurities[9,10] can plasmons be excited.

In this paper, an experiment is described in which thin Bi films (50—830 nm) have been illuminated with far-infrared radiation (FIR) in the spectral region covering the electron plasma frequency. The absorption and transmission have been measured as a function of frequency and film thickness. In films having a thickness in excess of 200 nm, a broad absorption band is observed around the plasma frequency. In thinner films, such an absorption is not present. This resonance results from an excitation of the electron gas in so-called virtual modes, which are damped by energy losses due to an outgoing electromagnetic plane wave. This damping is strongest in thin films, hence introducing a critical film thickness below which the resonance cannot persist.

Explicit calculations for the electrodynamics of a thin film on a substrate will show that a Drude model for the dielectric function is not sufficient to explain the experimental results in detail. The deviations will be analyzed in terms of a two-phonon absorption mechanism in a simplified model. Also, the influence of electron—ionized-impurity scattering on the experimental spectra will be discussed.

II. EXPERIMENT

A. Experimental setup

For the optical measurements in the far-infrared, a Grubb-Parsons-Michelson interferometer[11] was used in the spectral range from 25 to 225 cm^{-1}. Phase-sensitive detection was achieved by modulating the position of one of the interferometer mirrors at a frequency of 3 Hz.

The substrate with the deposited Bi film was mounted at the end of an oversized waveguide with the film facing the radiation perpendicularly. Simultaneously, the absorption, transmission, and background of the incoming radiation could be measured. Bolometers made of small chips of Allen-Bradly carbon resistors were used as detectors.

The reference bolometer used for the background measurements was mounted above the film but completely shielded from any reflected radiation. The absorption bolometer was thermally connected with the substrate and film via one of the electrical contacts attached to the film. This configuration allows the absorption to be measured in a direct way by the heating of the film. All radiation passing through the film was collected by a Winston-cone and absorbed by the transmission bolometer. The system with sample and detectors was under vacuum and immersed in a pumped ^{4}He bath kept at $T=1.6$ K. To provide appropriate sensitivity, the bolometers and sample were cooled by an additional ^{3}He system. In operation, the bolometers could be kept at $T=0.9$—1.3 K and the film, only cooled via the absorption bolometer, at $T=1.5$ K. Absorption and transmission signals were divided by the background signal and reduced to signals of approximately the same relative strength.

B. Sample fabrication

Single-crystal quartz plates cleaved perpendicularly to the z axis were used as a substrate. Apart from a narrow absorption line at $\simeq 134$ cm^{-1} this substrate material[12] shows no significant absorption for frequencies up to 230 cm^{-1}. One can therefore approximate the substrate by a nonabsorbing medium having a real refractive index $n=2.15$. To eliminate Fabry-Perot interference in the substrate, the thickness was made wedge-shaped going from 0.2 to 0.3 mm over a diameter of 15 mm.

Prior to the deposition of the Bi film, four Au contacts were deposited at symmetrical points on the periphery of the substrate to enable a dc square-resistance measurement in a van der Pauw[13] geometry. The Bi films were deposited by evaporation of 99.999% pure Bi on a quartz substrate at a residual gas pressure of 3×10^{-4} Pa. In order to improve the structure, the films were deposited in two steps.[14] The film thickness was measured using an optical interference method with an accuracy of 5–10%. Films were made and investigated in the thickness range from 50 to 830 nm.

The film structure was investigated by scanning electron microscopy (SEM) and x-ray diffraction. The latter showed a very strong crystal orientation of the trigonal crystal axis perpendicular to the film surface. The SEM work showed the films to be composed of grains having dimensions 1.5 to 4 times the film thickness. The films had considerable surface roughness and some protruding crystals at a false orientation, a feature which is commonly seen in evaporated Bi films.[15]

C. Bi properties

In spite of the fact that Bi is a semimetal with a complex band structure and Fermi surface,[16] the electrical properties can be described using rather few parameters as long as the experiments do not involve magnetic fields. In a semimetal conduction occurs through electrons and holes, but in Bi the electrons account for most of the conductivity owing to their very low effective mass ($m^*\simeq 0.01 m_e$) which is almost isotropic in spite of a very anisotropic mass tensor.[17,18] The electron density at low temperatures[19,20] is $n=3\times 10^{23}$ m^{-3}. The contribution from the bound charges to the optical properties is represented by ϵ_∞, the optical dielectric constant of the lattice.[1,21] At far-infrared frequencies, ϵ_∞ is essentially frequency independent with a value ranging from 60 to 100 for different crystal orientations.[4,18,22]

D. dc results

Using the van der Pauw geometry the dc resistance per square was measured at $T=1.5$ K and ranged from about 200 to 5Ω for increasing film thickness from 50 to 830 nm. After converting to the dc conductivity (σ_0) the electron scattering time τ was estimated from the Lorentz-Sommerfeld relation[2] [see Eq. (3)]. The scattering time ranged between 4×10^{-14} and 3×10^{-13} sec for increasing thickness of the investigated films. This is of the same order as found in other experiments.[9] From the Fermi energy[23] ($E_F=28$ meV) and the effective mass ($m^*=0.01 m_e$), the Fermi velocity can be calculated, which yields, in combination with the scattering time τ, a value for the electron mean free path l. For all films, l was of the order of the film thickness.

E. FIR results

In Figs. 1 and 2 the experimental results are plotted, respectively for the absorption and the transmission spectra of the Bi films as a function of the film thickness. Due to the absence of a sample having known absorption and transmission, no accurate absolute scales could be obtained. Some residual small-scale structures at the spectral ends are due to the normalization process which involves dividing by signals of very low intensity. To keep the picture surveyable all spectra have been shifted upwards an amount as indicated by the numbers in front of each curve.

Figure 1 clearly shows that for films thinner than 200 nm, the absorption is rather frequency independent, and that for increasing film thickness a very broad absorption band develops at 160 cm^{-1}. The transmission (Fig. 2) is also featureless for thin films and develops a shoulder at about 160 cm^{-1} with increasing film thickness. These results will be discussed in the next sections.

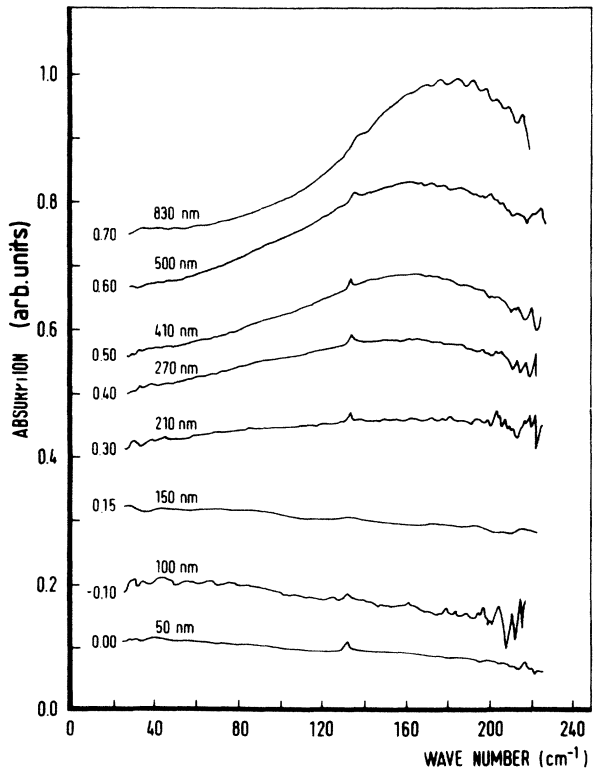

FIG. 1. The experimental far-infrared absorption of the Bi films at $T=1.5$ K. The film thickness is given in nm. The numbers in front of each spectrum indicate the real zero absorption on the ordinate scale. The small resonance at 134 cm^{-1} is due to a strong absorption line in the substrate.

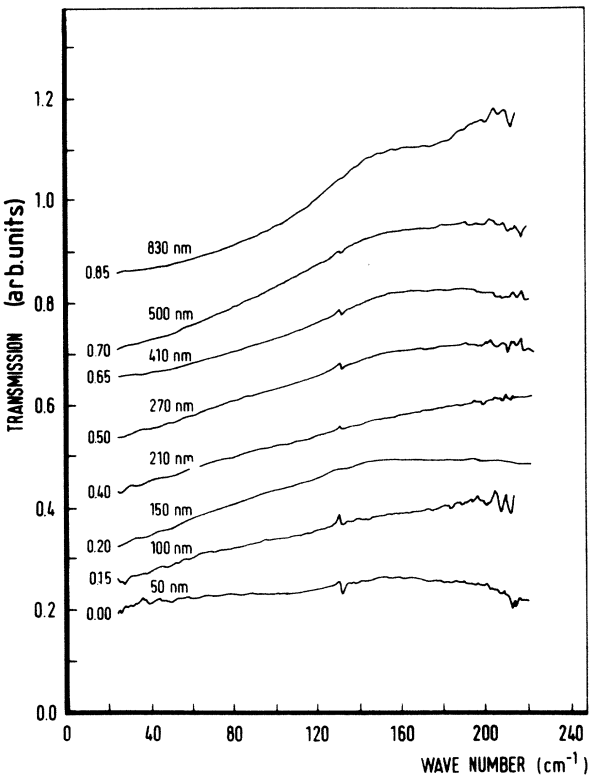

FIG. 2. The experimental far-infrared transmission of the Bi films at $T=1.5$ K. For this figure, the same comments as given in Fig. 1 are applicable.

III. ELECTRODYNAMICAL ANALYSIS

A. Introduction

At optical frequencies, the distinction between bound and free charges, which is very definite in dc cases, becomes less explicit. The usual method of describing the optical properties of a conducting solid is therefore to combine the dielectric permittivity and the free-electron contribution in a single effective dielectric function $\epsilon(\omega)$ defined[24] as

$$\epsilon(\omega)=\epsilon_\infty+\frac{i\sigma(\omega)}{\omega\epsilon_0}\ , \tag{1}$$

where ϵ_∞ is the dielectric contribution from the bound charges and $\sigma(\omega)$ the dynamical conductivity from the free-conduction electrons. ϵ_∞ is usually a constant up to frequencies far above the FIR. Likewise, an effective displacement current $\mathbf{D}$ is defined through $\mathbf{D}=\epsilon_0\epsilon(\omega)\mathbf{E}$ and as such, incorporates the free-electron current $\mathbf{J}$. At an interface in the absence of surface charges, the correct boundary conditions[24,25] are given by the continuity of the tangential electromagnetic fields $\mathbf{E}$ and $\mathbf{B}$ and of the normal displacement current $\mathbf{D}$.

As a first approximation, the dynamical conductivity will be used in the Drude model

$$\sigma(\omega)=\frac{\sigma_0}{1-i\omega\tau}\ , \tag{2}$$

with the electronic relaxation time τ and the dc conductivity σ_0 given by the Lorentz-Sommerfeld relation

$$\sigma_0=\frac{ne^2\tau}{m^*}\ , \tag{3}$$

in which n is the electron density and m^* the effective electron mass. Using the screened-electron plasma frequency ω_{p^*} given by

$$\omega_{p^*}^2=\frac{ne^2}{m^*\epsilon_0\epsilon_\infty}\ , \tag{4}$$

the dielectric function $\epsilon(\omega)$ is written as

$$\epsilon(\omega)=\epsilon_\infty\left[1-\frac{\omega_{p^*}^2}{\omega^2+i\omega\omega_\tau}\right]\ , \tag{5}$$

with the collision frequency $\omega_\tau=1/\tau$.

B. Virtual modes

Although the presence of a substrate has a non-negligible influence on the optical response of the system, neglecting the substrate in the calculations will still yield results that preserve the principal features of the experiment. Therefore, in order to understand the nature of the observed thickness dependent resonances, we will present in this section the electrodynamics of a thin film bounded by vacuum on both sides.

Suppose a film in the $(\hat{x},\hat{y})$ plane having a thickness ranging from $-a$ to $+a$ in the $\hat{z}$ direction and characterized by a dielectric function as given by Eq. (1). Of most interest are solutions of the Maxwell equations which are only periodical in the plane of the film and of the form

$$\mathbf{E}=\mathbf{E}(z)e^{i(k_x x-\omega t)},\quad \mathbf{B}=\mathbf{B}(z)e^{i(k_x x-\omega t)}\ . \tag{6}$$

Kliewer and Fuchs[26–28] have shown that for this problem the solutions of the Maxwell equations can be divided in two types: radiative and nonradiative modes. The latter are optically inactive. The former modes involve outgoing plane waves radiating away energy from the film at an angle θ with the normal of the film given by $\sin\theta=|k_x/k|$, provided $k_x^2<k^2=\omega^2/c^2$. These solutions are optically active and as such relevant to our experiment. Because of the energy loss due to radiation damping these modes are not stationary, and are therefore often referred to as virtual modes.

Applying the correct boundary conditions, Kliewer and Fuchs have shown that a virtual mode can be present at a frequency given by the virtual-mode equation,

$$\epsilon(\omega)=-i\frac{\kappa}{\kappa_0}\cot(\kappa a)\ , \tag{7}$$

with $\kappa^2=\epsilon(\omega)k^2-k_x^2$, and $\kappa_0^2=k^2-k_x^2$. The solutions of Eq. (7) are complex frequencies $\omega=\omega_1+i\omega_2$ of which the real part represents the resonance frequency, and the imaginary part a frequency spread. It can be shown[26–28] that the absorption caused by these modes has roughly a Lorentzian line shape at ω_1 with a width ω_2 provided $|\omega_2/\omega_1|<1$.

For the experimental situation with perpendicular in-

cident light (limit $k_x \rightarrow 0$), we have calculated the virtual-mode frequencies in Bi films for several values of the electronic relaxation time τ by inserting Eq. (5) into Eq. (7). The virtual-mode frequency is normalized to the screened-plasma frequency ω_{p*} and plotted in Fig. 3 as a function of the film thickness. Using the relevant experimental parameters according to Sec. II C, ω_{p*} equals approximately 164 cm^{-1}. Unity on the dimensionless thickness scale in Fig. 3 represents a Bi film of about 100 nm thickness. From Fig. 3, we expect to see a very broad resonance at the screened-plasma frequency for films with a thickness in excess of 150 nm, which is compatible with the experimental results in Fig. 1. Figure 3 also reveals that damping due to electron scattering is only of minor importance as far as the resonance frequency is concerned.

C. Energy-loss aspect

In the preceding section, it was shown that optically active lateral oscillations can only be present around the plasma frequency in films exceeding a critical film thickness. Qualitatively, this can be understood using the concept of energy content and energy loss.

The solution of the Maxwell equations is a nearly homogeneous electric field in the plane of the film which varies harmonically in time. This field has a time-averaged energy content $W = \mathrm{Re}(\mathbf{E}\cdot\mathbf{D})$ per unit area given by

$$W(d) = \epsilon_0 \mathrm{Re}[\epsilon(\omega)] E_x^2 d \ , \tag{8}$$

for a film with thickness d. Only in the case of vanishing $\mathrm{Re}[\epsilon(\omega)]$ a strong electric field an be present at a low-energy content. This is a way to see why a virtual mode oscillates preferably near the plasma frequency.

The continuity of E_x across the film-vacuum interface determines the amplitude of the outgoing plane wave. Per unit area, the energy transport P_r out of the film will be

$$P_r = \epsilon_0 c E_x^2 \ . \tag{9}$$

In the absence of electron scattering energy conservation connects the stored energy $W(d)$ with the energy transport P_r in the following way:

$$\frac{d}{dt} W(d) = -P_r \ . \tag{10}$$

This expression reveals that an oscillation initiated at a certain moment decays exponentially with a decay time τ_r given by

$$\tau_r = \frac{\mathrm{Re}[\epsilon(\omega)] d}{c} \ . \tag{11}$$

According to Fourier theory, such a decay time causes a frequency spread $\Delta\omega$ given by $\Delta\omega\tau_r \simeq 1$. Therefore, for an oscillation close to the plasma frequency, the following relation can be derived from Eq. (11):

$$\frac{\Delta\omega}{\omega} \simeq \frac{d^*}{d} \ , \tag{12}$$

where d^* represents a critical film thickness given by

$$d^* = \frac{c}{\omega_{p*}\epsilon_\infty} \ . \tag{13}$$

In this derivation, the assumption has been made that around the plasma frequency $\mathrm{Re}[\epsilon(\omega)]$ will be of the order of ϵ_∞, which makes d^* just a rough estimate. Equation (12) reveals immediately that for a well-defined resonance, the film thickness should be in excess of d^* (which is close to 100 nm in Bi). The expression given in Eq. (12) equals the imaginary part of the virtual-mode frequency as can be calculated from Eq. (7), assuming zero electron scattering. d^*, as given in Eq. (13), is also used as the scaling factor on the abscissa of Fig. 3.

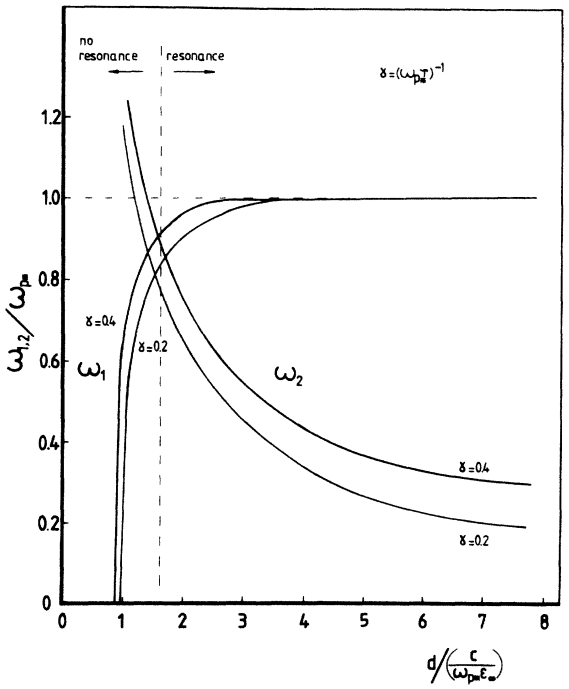

FIG. 3. The complex virtual-mode frequency in a thin film as a function of a dimensionless film thickness. The frequencies are normalized on the theoretical screened-plasma frequency ω_{p*}, and calculated for two values of the electronic relaxation time τ represented by the parameter γ. The vertical dashed line marks the critical film thickness below which the resonance disappears by virtue of a too large imaginary frequency. Applied to Bi, unity on the abscissa represents a film thickness of approximately 100 nm.

D. Optical response

To obtain the actual shape of the optical-absorption and transmission spectra, the virtual modes must be coupled explicitly to an incoming, a reflected, and a transmitted wave.[27] The general way to perform such a calculation is to express the fields inside the film in the fields on both sides of the film using the Maxwell equations, giving expressions for the power transmission (T) and reflection (R). The absorption (A) if defined by virtue of energy conservation as $A = 1 - T - R$.

To compare theory and experiment in detail, it is neces-

sary to include the presence of the substrate in the calculations. Even a perfectly nonabsorbing substrate can have a non-negligible influence on the detailed frequency dependence and magnitude of the reflection, absorption, and transmission, due to its large refractive index. This originates in the impedance matching[29] which exists between the film, the substrate, and the vacuum. Because of this influence, we have employed the expressions derived by de Kort *et al.*[29] for the optical properties of a film supported on a substrate. Following the notation in their paper, T, and R are given by[30]

$$T=\left|\frac{\alpha}{\beta}\right|^2, \quad A=\left|\frac{\gamma}{\beta}\right|^2, \tag{14}$$

with

$$\alpha=i\omega c(F_1^+-F_1^-)(F_2^+-F_2^-), \tag{15a}$$

$$\begin{aligned}\beta=&(F_1^++F_1^-)(\omega^2F_2^+F_2^--c^2)\\&+(F_2^++F_2^-)(\omega^2F_1^+F_1^--c^2)\\&+i\omega c(F_1^++F_1^-)(F_2^++F_2^-)\\&+2i\omega c(F_1^+F_1^-+F_2^+F_2^-),\end{aligned} \tag{15b}$$

$$\begin{aligned}\gamma=&(F_2^++F_2^-)(\omega^2F_1^+F_1^-+c^2)\\&+(F_1^++F_1^-)(\omega^2F_2^+F_2^-+c^2)\\&+2i\omega c(F_1^+F_1^--F_2^+F_2^-),\end{aligned} \tag{15c}$$

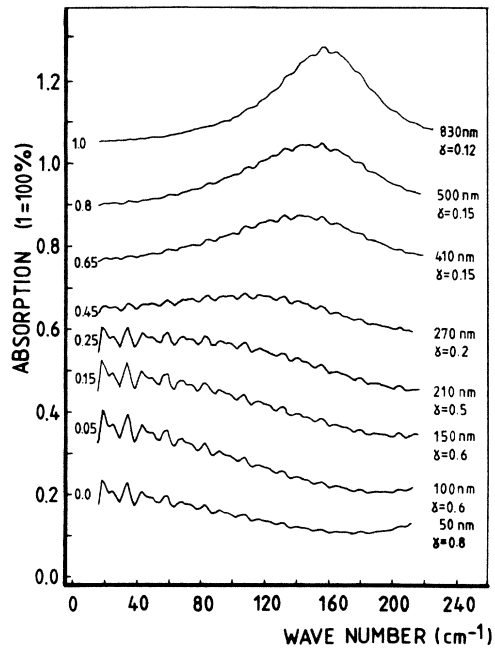

FIG. 4. The theoretical far-infrared absorption of thin Bi films on a wedge-shaped quartz substrate calculated in the Drude approximation. The film thickness is given in nm and the numbers in front of each spectrum indicate the real zero on the ordinate. The electronic relaxation rate is presented by $\gamma=1/\omega_{p*}\tau$. The parameters used for the calculation are $m^*/m_e=0.01$, $\epsilon_\infty=100$, $n=3\times10^{23}$ m^{-3}, $\omega_{p*}=164$cm^{-1}, $n_{\text{quartz}}=2.15$.

and with

$$\begin{aligned}F_i^+&=\frac{-1}{k(\epsilon_i)^{1/2}}\cot[ka_i(\epsilon_i)^{1/2}],\\F_i^-&=\frac{1}{k(\epsilon_i)^{1/2}}\tan[ka_i(\epsilon_i)^{1/2}].\end{aligned} \tag{16}$$

In these equations, the index $i=1$ refers to the medium facing the radiation, which is the Bi film in our experiment. The index $i=2$ consequently refers to the substrate.

In the calculations, the following substitutions are made in Eqs. (14)–(16): ϵ_1 according to Eq. (5) with the Bi-parameters from Sec. II C, the scattering time τ as calculated from the dc square resistance values, and the film thickness $2a_1$. The refractive index of the substrate n is substituted in $\epsilon_2=n^2$ and the substrate thickness is $2a_2$. The results for the absorption and the transmission of this model calculation in the Drude approximation are presented in Figs. 4 and 5 in which the scattering time τ is represented by the parameter $\gamma=1/\omega_p^*\tau$. To include the wedge shape of the substrate the computer program integrates over the substrate thickness in discrete steps which leaves some residual small-scale structure in the theoretical spectra.

Inserting $\epsilon_2=1$ into Eqs. (14)–(16) revealed that the main effect of the substrate on the absorption is a considerable smoothing and broadening effect on the resonance, especially at the high-frequency side. The overall absorption was also strongly reduced by the presence of the substrate. Similar non-negligible effects were found concerning the transmission.

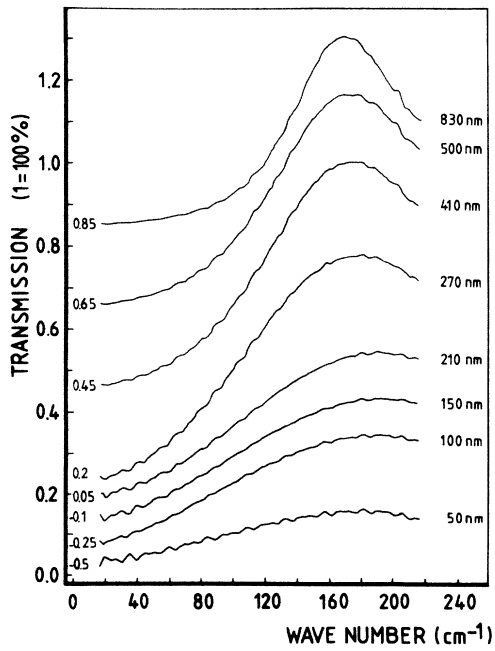

FIG. 5. The theoretical far-infrared transmission of the Bi films on a wedge-shaped quartz substrate calculated in the Drude approximation. For this figure the same comments as given in Fig. 4 are applicable.

E. Comparison between Drude model and experiment

The theoretical absorption in Fig. 4 reveals a frequency and thickness dependence which differs considerably from the experimental absorption in Fig. 1. Firstly, in the experiment the resonance does not shift towards lower frequencies for thinner films. Secondly, the experimental resonance is broad compared with the theory.

A striking difference exists between the experimental and the theoretical transmission (Figs. 2 and 5). The predicted maximum in the transmission around ω_p* is observed as a shoulder in the experiment. This particularly strong deviation is the most important evidence that the Drude approximation is not sufficient to describe the far-infrared properties of thin Bi films in detail. In the next sections, several mechanisms will be discussed to explain the apparent discrepancy between the experiment and the Drude theory.

F. Deviations from the Drude model

1. Nonlocal effects

From the expressions for $\epsilon(\omega)$, one can calculate the skin-depth δ to be of order of 5—20 μm in the frequency region of interest. This value is in excess of the electron mean free path and of the film thickness. Hence electrodynamics are not yet in the anomalous regime[2,3] and it is justified to use local relations between fields and currents.

2. Two-phonon processes.

The influence of optical-phonon resonances can be investigated by the dielectric function

$$\epsilon(\omega)=\epsilon_\infty+\chi_{fc}+\chi_{\rm ph}\ , \tag{17}$$

in which χ_{fc} represents the free-electron contribution given by the frequency-dependent part of Eq. (5), and $\chi_{\rm ph}$ the susceptibility caused by the optical phonons. In the classical approximation, $\chi_{\rm ph}$ is given by

$$\epsilon_\infty+\chi_{\rm ph}=\epsilon_\infty\frac{\omega_L^2-\omega^2-i\omega\Gamma}{\omega_T^2-\omega^2-i\omega\Gamma}\ , \tag{18}$$

where ω_L is the longitudinal-optical- (LO) phonon frequency, ω_T the transversal-optical- (TO) phonon frequency, and Γ the damping. The dielectric function, according to Eq. (18), is presented in Fig. 6. Using the full expression for the dielectric function the theoretical absorption and transmission have been calculated using Eqs. (14)—(17). For an optimal match between theoretical and experimental spectra, the following parameter values have been used: $\epsilon_\infty=90\pm5$, $\omega_T=205\pm5$ cm^{-1}, $\omega_L=220\pm10$ cm^{-1}, and $\Gamma=150\pm50$ cm^{-1}. The results for the calculated absorption and transmission are shown in Figs. 7 and 8. The experimental data agree fairly well with these calculations, except for an unexplained bulge in the measured high-frequency transmission of the thickest film.

As Bi has a rhombohedral[31] crystal structure with two atoms in each unit cell the first-order fundamental lattice absorption is not infrared active because the (zone-centered) optical phonons produce no electric dipole field.[5,6] Using Raman scattering,[31,32] the optical-phonon frequencies near the zone-center are established as 75

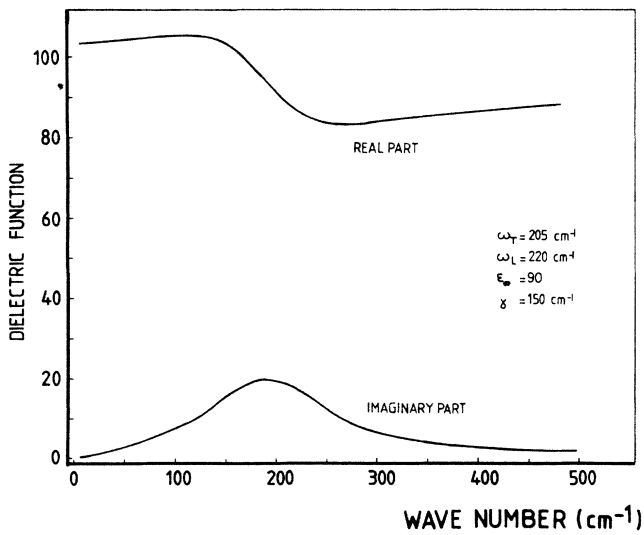

FIG. 6. The contribution from the lattice to the dielectric function corresponding to Eq. (18). The presented parameters yield a good theoretical description of the experimental absorption and transmission.

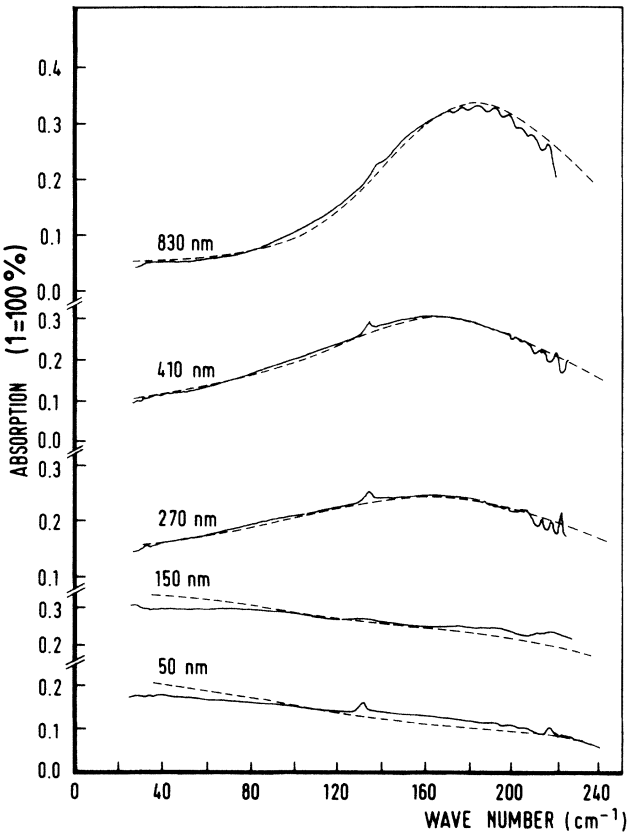

FIG. 7. The experimental absorption of the Bi films compared with the theoretical model (dashed line) including the phonon contribution as given by Eqs. (17) and (18). The calculation includes the wedge-shaped substrate and has been smoothed to dispose of some residual Fabry-Perot interferences.

cm^{-1} (TO) and 100 cm^{-1} (LO). MacFarlane[33] has obtained the wave-vector-dependent optical-phonon branches along the trigonal crystal axis from neutron diffraction. The frequencies range from 75 to 102 cm^{-1} (TO branch) and from 100 to 108 cm^{-1} (LO branch). Therefore the frequencies ω_T and ω_L in Eq. (18) seem to arise from a summation band, i.e., a two-phonon process.

As the wave vectors of the two phonons can cancel each others momentum no restriction to zone-centered phonons has to be made, thus allowing for a frequency spread[34] in the two-phonon absorption band. Lax and Burnstein[35] have proposed a two-phonon absorption mechanism involving second-order terms in the electric moment produced by charge deformations on the scale of the lattice constant. As such, this mechanism favors short-wavelength phonons and hence absorption will arise mainly from a pair of zone-boundary phonons. According to the neutron-diffraction data of the optical phonons,[33] two-phonon absorption in Bi is expected to occur in the region between 200 and 220 cm^{-1}.

A detailed calculation performed by Cowley[36] indicates that the two-phonon contribution has, in a smoothed form, a distinct resemblance to the plot presented in Fig. 6. In two-phonon processes the dielectric susceptibility $\chi_{2ph}(\omega)$ resembles a self-convolution of $\chi_{ph}(\omega)$ according to

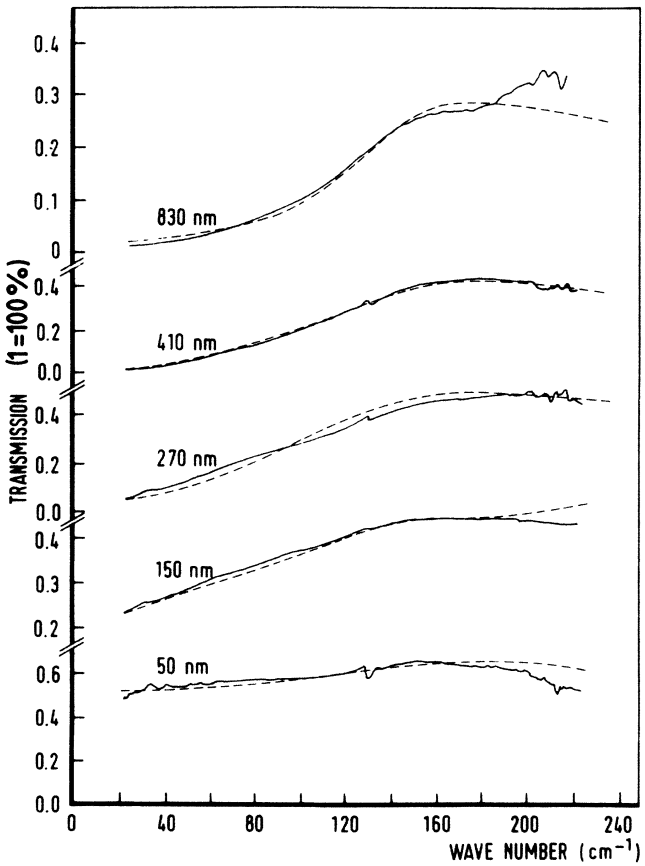

FIG. 8. The experimental transmission of the Bi films compared with the theoretical model (dashed line) including the phonon contribution. For this figure the same comments as given in Fig. 7 are applicable.

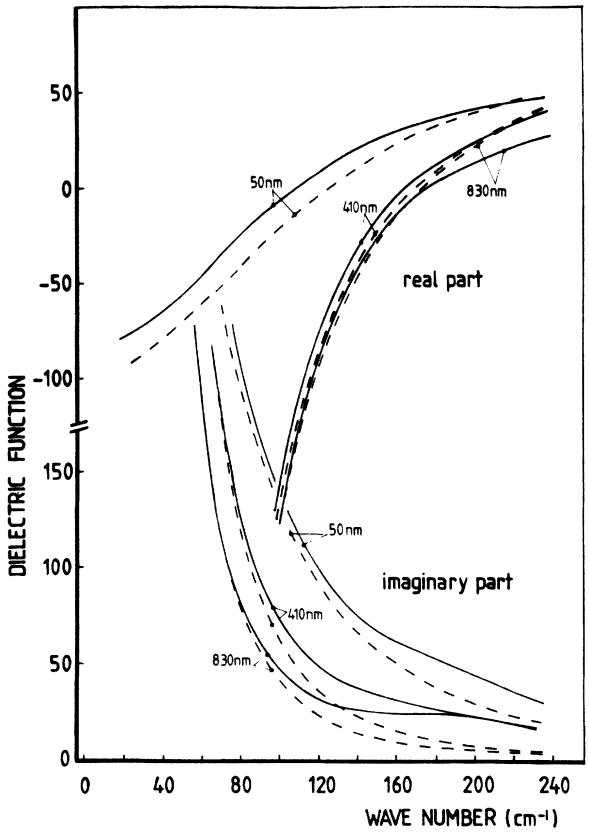

FIG. 9. The dielectric function of Bi films of various film thickness. The solid line presents the dielectric function including the two-phonon contribution. The Drude model dielectric function is given by a dashed line.

$$\chi_{2ph}(\omega) \propto \int \chi_{ph}(\omega_1)\chi_{ph}(\omega-\omega_1)d\omega_1 \,. \tag{19}$$

The result of such a self-convolution is roughly a strong smoothing and a doubling of the arguments of the involved function. Therefore it is reasonable to approximate the two-phonon contribution by a single-phonon process as in Eq. (18), including a strong damping and doubled resonance frequencies (depicted in Fig. 6).

3. *Electron-impurity scattering*

Figure 9 presents the dielectric function used to obtain the theoretical-absorption and transmission spectra depicted in Figs. 7 and 8, and gives a comparison with the Drude model. To keep the picture surveyable, not all films involved in the experiment have been included. As is obvious from Figs. 7 and 8, this dielectric function describes the investigated films rather well.

A similar deviation from the Drude model as observed in Fig. 9 has been derived in Ref. 9 from reflection measurements on bulk Bi between 50 and 500 cm^{-1}. This phenomenon is ascribed to the scattering of conduction electrons by ionized impurities which causes the collision time τ to become frequency dependent. We will give an overview of the main points of this theory and make a comparison with our experimental results.

In the Drude approximation, the dynamical resistivity

$\rho(\omega)$ has the form

$$\rho(\omega)=\frac{\omega_\tau}{\epsilon_0\omega_p^2}-\frac{i\omega}{\epsilon_0\omega_p^2}\ , \tag{20}$$

in which ω_p is the unscreened plasma frequency. Only the real part of $\rho(\omega)$ depends on electron scattering and is frequency independent. A more realistic scattering theory results in

$$\rho(\omega)=\hat{\rho}(\omega)-\frac{i\omega}{\epsilon_0\omega_p^2}\ , \tag{21}$$

where $\hat{\rho}(\omega)$ will be necessarily complex[10] and contains the frequency-dependent scattering mechanisms. Any observed frequency dependence in the real part of the dynamical resistivity $\rho(\omega)$ indicates a deviation from the Drude model.

The influence of electron—ionized-impurity scattering can be visualized as follows.[9,10,37] In principle, real plasmons (i.e., longitudinal charge density fluctuations having $\nabla\cdot\mathbf{E}\neq 0$) cannot be induced by a transversal electromagnetic wave ($\nabla\cdot\mathbf{E}=0$). The spherical field of a screened ionized impurity can, however, break the transversal symmetry and thus allows for a longitudinal component in the total electric field. Above the screened plasma frequency, real plasmons can now be excited. Through these plasmons, energy is dissipated from the incident radiation which yields a strong increase of the absorption, and hence of ω_τ. Due to plasmon decay in single-particle excitations (Landau damping[1,38]) plasmons can only exist in a small frequency region above ω_{p*}.

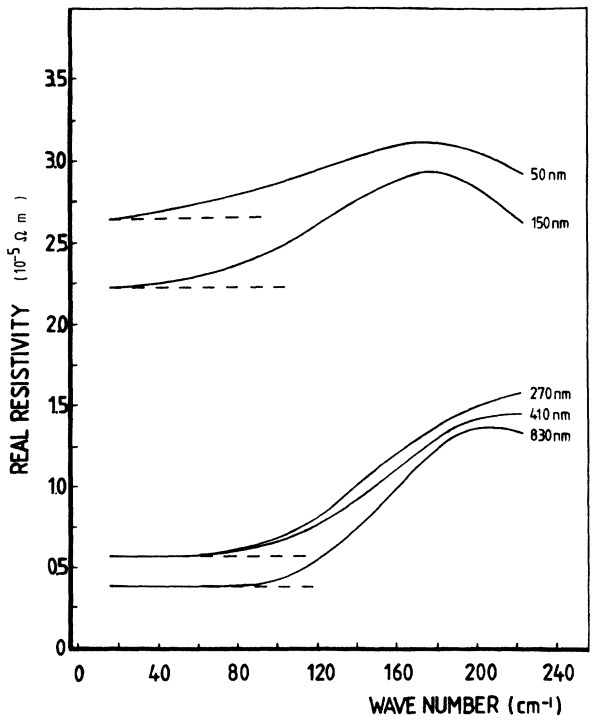

FIG. 10. The real part of the resistivity of the Bi films (solid line). The Drude contribution which is frequency independent is indicated by a dashed line.

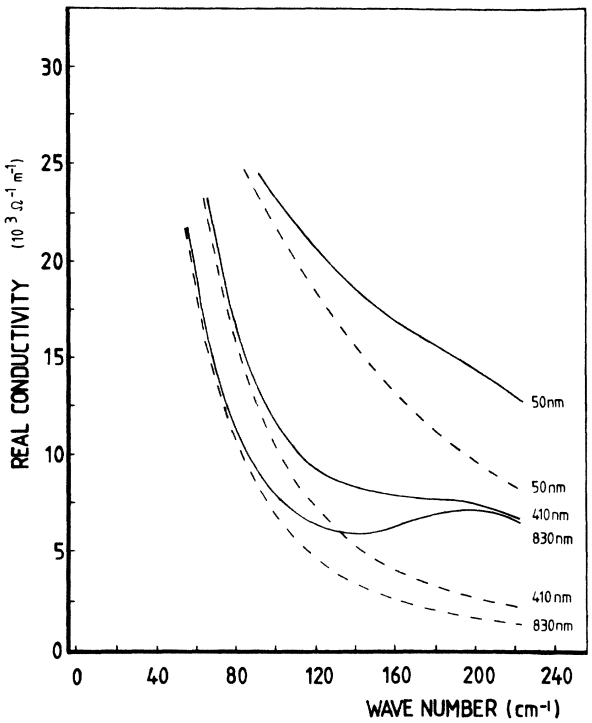

FIG. 11. The real part of the conductivity of the Bi films (solid line). The Drude conductivity is given by a dashed line.

Therefore, for high frequencies of the incident light, the plasmons will have no phase correlation with the rapidly oscillating electromagnetic field and absorption (and ω_τ) will be strongly reduced. Quantitatively, the model including the electron—ionized-impurity scattering results in a strong peak in the real resistivity rising a factor 5 to 10 in magnitude over the Drude resistivity in the region from ω_{p*} to $4\omega_{p*}$, followed by a power-law decrease up to high frequencies. A similar behavior is predicted to occur in the optical conductivity.

The effect of ionized-impurity scattering on the dielectric function in Bi has been calculated by Gerlach, Grosse, Rautenberg, and Senske.[9] To compare our experimental results with these calculations, we have determined the real part of the resistivity and the optical conductivity of the investigated films by substituting the dielectric function from Fig. 9 into Eq. (1). The results are presented in Figs. 10 and 11, together with the data according to the Drude model. If one compares the results presented in Figs. 10 and 11 with the calculations in Ref. 9, a qualitative agreement between experiment and theory is found. Quantitatively, however, the deviations from the Drude model as observed in our experiment become already appreciable at frequencies considerably below the plasma frequency ω_{p*} which cannot be accounted for by the impurity-scattering theory.

IV. CONCLUSION

In conclusion, we have shown that around the plasma frequency, a broad thickness-dependent optical resonance

is present in thin Bi films illuminated with far-infrared radiation. This resonance is purely transversal and can be partly described by a screened free-electron gas in the Drude approximation.

Deviations from the simple Drude model can be explained by either two-phonon processes or by electron–ionized-impurity scattering. The first mechanism yields a very good agreement between theory and experiment, whereas impurity scattering can account for the experimental results in a qualitative way.

The experiments show that despite of the fairly rough films and their complex anisotropic properties, the Bi layers can be nicely approximated with a flat homogeneous isotropic film having bulk properties.

ACKNOWLEDGMENTS

The authors wish to thank Dr. A. P. van Gelder and Dr. H. Sigg for the valuable discussions on the electrodynamics of thin films. Dr. W. J. Kaal receives our appreciation for preliminary work on the experimental setup. We are greatly indebted to Professor Grosse from the Technical University of Aachen for drawing attention to the electron–ionized-impurity scattering mechanism.

---

*Present address: Hochfeld-Magnetlabor, Max-Planck-Institut für Festkörperforschung, 25 avenue des Martyrs, 166X, F-38042 Grenoble Cédex, France.

[1]D. Pines, *Elementary Excitations in Solids* (Benjamin, New York, 1964).

[2]H. E. Bennet and J. E. Bennet, in *Proceedings of the International Colloquim on the Optical Properties and Electronic Structure of Metals and Alloys—1965 (Paris),* edited by F. Abelès (North-Holland, Amsterdam, 1966), p. 175–188.

[3]G. E. H. Reuter and E. H. Sondheimer, Proc. R. Soc. London, Ser. A **195**, 336 (1948).

[4]W. S. Boyle and A. D. Brailsford, Phys. Rev. **120**, 1943 (1960).

[5]R. Zallen, Phys. Rev. **173**, 824 (1968).

[6]R. N. Zitter and P. C. Watson, Phys. Rev. B **10**, 607 (1974).

[7]R. H. Ritchie, Surf. Sci. **34**, 1 (1973).

[8]G. Rasigni, J. P. Palmari, and M. Rasigni, Phys. Rev. B **12**, 1121 (1975).

[9]E. Gerlach, P. Grosse, M. Rautenberg, and W. Senske, Phys. Status Solidi B **75**, 533 (1976).

[10]E. Gerlach and P. Grosse, in *Festkörperprobleme XVII: Advances in Solid State Physics,* edited by J. Treusch (Vieweg, Dortmund, 1977), pp. 157–193.

[11]G. W. Chantry, M. M. Evans, J. Chamberlain, and H. A. Gebbie, Infrared Phys. **9**, 85 (1969).

[12]E. V. Loewestein, D. R. Smith, and R. L. Morgan, Appl. Opt. **12**, 398 (1973).

[13]L. J. van der Pauw, Philips Tech. Rev. **20**, 221 (1958/59).

[14]K. Abdelmoula, B. Parolo, C. Pariset, and D. Rinard, Thin Solid Films **62**, 273 (1979).

[15]A. Barna, P. B. Barna, R. Fedorowich, G. Radnoczi, and H. Sugawara, Thin Solid Films **36**, 75 (1976).

[16]M. S. Dresselhaus, in *The Physics of Semimetals and Narrow-gap Semiconductors—1970 (Dallas),* proceedings of the conference, edited by D. L. Carter, and R. T. Bate (Pergamon, Oxford, 1971), p. 3.

[17]R. N. Zitter, Phys. Rev. **127**, 1471 (1962).

[18]A. A. Cottey, J. Phys. C **8**, 4135 (1975).

[19]Yu. F. Komnik, E. I. Bukhshtab, Yu. F. Nikitin, and V. V. Andrievskii, Zh. Eksp. Teor. Fiz. **60**, 669 (1971) [Sov. Phys.—JETP **33**, 364 (1971)].

[20]J. M. Noothoven van Goor, Philips Res. Rep. Suppl. **4**, 1 (1971).

[21]R. Schuchhardt, R. Rudolph, R. Keiper, and H. Krüger, Phys. Status Solidi B **97**, 257 (1980).

[22]C. Nanney, Phys. Rev. **129**, 109 (1963).

[23]R. L. Blewitt and A. J. Sievers, J. Low Temp. Phys. **13**, 617 (1973).

[24]A. R. Melnyk and M. J. Harrison, Phys. Rev. B **2**, 835 (1970).

[25]A. R. Melnyk, in *Polaritons—1972 (Taormini),* proceedings of the First Taormini Research Conference on the Structure of Matter, edited by E. Burnstein and F. de Martini (Pergamon, New York, 1972) pp. 221–228.

[26]K. L. Kliewer and R. Fuchs, Phys. Rev. **150**, 573 (1966).

[27]R. Fuchs, K. L. Kliewer, and J. Pardee, Phys. Rev. **150**, 589 (1966).

[28]K. K. Kliewer and R. Fuchs, Phys. Rev. **153**, 498 (1967).

[29]C. G. C. M. de Kort, J. H. M. Stoelinga, and P. Wyder, Physica **101B**, 1 (1980)

[30]In Ref. 29, several expressions not affecting the results should be corrected as follows. Eq. 2.13, expression for E': $cE_2^-/i\omega F_2^-$ must be preceded by a minus sign. Eq. 2.14 expression for α: $F_1^+ + F_1^-$ should read $F_1^+ - F_1^-$. Eq. 2.17: F_1^+ and F_1^- should be interchanged. Eq. 2.19: F_2^- and F_2^+ should be interchanged.

[31]R. N. Zitter, in *The Physics of Semimetals and Narrow-gap Semiconductors,* Ref. 16, pp. 289–295.

[32]W. B. Grant, H. Schulz, S. Hüfner, and J. Pelzl, Phys. Status Solidi B **60**, 331 (1973).

[33]R. E. MacFarlane, in *The Physics of Semimetals and Narrow-gap Semiconductors,* Ref. 16, p. 289.

[34]W. G. Spitzer, in *Semiconductors and Semimetals,* edited by R. K. Willardson and A. C. Beer (Academic, New York, 1967), Vol. 3, p. 17.

[35]M. Lax and E. Burnstein, Phys. Rev. **97**, 39 (1955).

[36]R. A. Cowley, Adv. Phys. **12**, 421 (1963).

[37]P. Grosse, in *Recent Developments in Condensed Matter Physics,* edited by J. T. Devreese (Plenum, New York, 1981), Vol. 1, p. 783.

[38]O. Madelung, *Introduction to Solid-State Theory* (Springer-Verlag, New York, 1978), Sec. 2.1.